Cyclic Plastic Deformation Behaviour of SA 312 Type 304LN Stainless Steel

Avinash Ethirajan, M. Saravanan, S. Vishnuvardhan, J. Jeyanthi

Abstract— **Many engineering components are often subjected to cyclic load excursions beyond elastic limit and hence cyclic plastic deformation in such components becomes inevitable. Since the resultant elastic-plastic stress-strain response of the material plays a pivotal role in analysis, design and failure of the component, it becomes important to understand the cyclic plastic deformation behaviour. Strain-controlled fatigue is an important consideration in the design of components that undergo either mechanically or thermally induced cyclic plastic strains which may cause failure in low number of cycles (approximately <105). This paper presents the details of strain-controlled low cycle fatigue tests carried out on SA 312 Type 304LN stainless steel material. ASTM E 606 - 12 was followed in preparing the test specimens and carrying out the fatigue tests. The tests were carried out under constant amplitude cyclic triangular waveform loading. The specimens were tested at six different strain amplitudes of ±1.10%, ±1.25%, ±1.40%, ±1.55%, ±1.70% and ±1.85%. Cyclic stress-strain hysteresis curves were obtained throughout the entire duration of the fatigue tests. The number of cycles to failure of the specimens was recorded. Using the empirical relationships, fatigue parameters, namely cyclic strength coefficient, cyclic strain hardening exponent, fatigue strength coefficient, fatigue strength exponent, fatigue ductility coefficient and fatigue ductility exponent were evaluated; the values of the same were found to be 414.66 MPa, 0.2048, 777.54 MPa, -0.1010, 0.1955 and -0.4780 respectively. These fatigue parameters will be useful in determining the number of fatigue loading cycles for fatigue-ratcheting crack initiation in components made of this material..**

Index Terms— **SA 312 Type 304LN stainless steel; strain-controlled fatigue test; cyclic plastic deformation; hysteresis curve; fatigue parameters.**

I. INTRODUCTION

Fatigue becomes an important consideration in the design of structures and components subjected to repetitive loading, e.g., power plants, chemical industries, offshore structures, machinery components and bridge structures. If the structure or component receives high stress cycles and the deformation is largely plastic, there is a possibility of low cycle fatigue failure, i.e., failure within a small number of cycles (approximately $<10^5$). When a material is subjected to earthquake type cyclic loading (an example of low cycle fatigue problem), the loading is followed by unloading and subsequent reloading, the material response may change cycle by cycle until it gets saturated. Other examples of low cycle fatigue where the study of strain controlled fatigue behaviour becomes important are: (i) thermal cycling where a component expands and contracts in response to fluctuations in the operating temperature, and (ii) high amplitude reversed bending between fixed displacements [1-3]. The extent of low cycle fatigue damage is influenced by stress concentrations (due to geometrical and material discontinuities, surface roughness, macro and micro inclusions and defects), type of loading (strain- or stress-controlled and degree of non-proportionality) and the presence of residual stresses (from manufacturing processes, prior large deformations and welding). Under inelastic load reversals, fatigue failure may involve progressive accumulation of deformation or strain (known as ratcheting) within plastically deformed zones. The presence of ratcheting during cyclic loading may reduce the crack initiation life and thus the fatigue life of components [4-6]. Inelastic material behaviour in closed loading path, repeated number of times, is known as cyclic plasticity. Experimental observations show a number of related phenomena. These are (i) Bauschinger effect, (ii) cyclic hardening (iii) cyclic softening, and (iv) ratcheting [7-10]. Some materials also show S-D (strength differential) effect [8].

This paper presents strain-controlled fatigue studies carried out on SA 312 Type 304LN stainless steel; based on the studies, cyclic behaviour of the material was studied and fatigue parameters were determined.

II. MATERIAL PROPERTIES

Material used in the present studies was SA 312 Type 304LN stainless steel conforming to ASTM A 312/ 312 M -14 [11]. The chemical composition of the material and the specified values as per ASTM A 312 / A 312 M - 14 standard are given in Table I. Mechanical properties of the material were determined by carrying out tension tests as per ASTM E 8M - 13a [12]. The average yield strength and ultimate tensile strength of the material were found to be 251 MPa and 611 MPa respectively. The modulus of elasticity and percentage of elongation of the material were found to be 183 GPa and 68 respectively.

TABLE I. CHEMICAL COMPOSITION OF SA 312 TYPE 304LN STAINLESS STEEL

Element	% weight (Tested)	ASTM A312/ A312M - 14 [2]

Avinash Ethirajan, M.E. Student, Department of Civil Engineering, Mepco Schlenk Engineering College, Sivakasi - 626 005, India.

M. Saravanan, Scientist, CSIR - Structural Engineering Research Centre, Council of Scientific and Industrial Research Centre, Taramani, Chennai, India.

S. Vishnuvardhan, Scientist, CSIR - Structural Engineering Research Centre, Council of Scientific and Industrial Research Centre, Taramani, Chennai, India.

J. Jeyanthi, Assistant Professor, Department of Civil Engineering, Mepco Schlenk Engineering College, Sivakasi - 626 005, India.

Carbon	0.025	0.035
Manganese	1.790	2.000
Phosphorus	0.022	0.045
Sulphur	<0.001	0.030
Silicon	0.357	1.000
Chromium	18.980	18.000 - 20.000
Nickel	9.350	8.000 - 12.000

III. Strain Controlled Fatigue Studies

Strain-controlled fatigue is an important consideration in the design of components that undergo either mechanically or thermally induced cyclic plastic strains which may cause failure in low number of cycles (approximately $<10^5$). Strain-controlled fatigue studies were carried out on SA 312 Type 304LN stainless steel. ASTM E606 / E606M - 12 : "Standard test method for strain-controlled fatigue testing" [13] was followed in preparing the test specimens and carrying out the fatigue tests. The test specimens were fabricated from a straight pipe of 168 mm nominal OD and 14 mm wall thickness. Initially, pipe to a length of 200 mm was cut from a straight pipe using hydraulic power hack saw; the specimens were then obtained from this cut portion along the length direction using Plasma Arc (PA) cutting and machining. Circular specimens having uniform-gauge test section and straight sided collet-grip end connections were chosen for the studies. The test specimens had overall dimensions of length 150 mm and diameter 13 mm; the diameter in the gauge section was 6.5 mm. Fig. 1 shows the details of low cycle fatigue test specimen.

The tests were carried out under strain control, using a ±250 kN capacity fatigue rated UTM. Fig. 2 shows the set-up for strain-controlled fatigue test and Fig. 3 shows the close-up

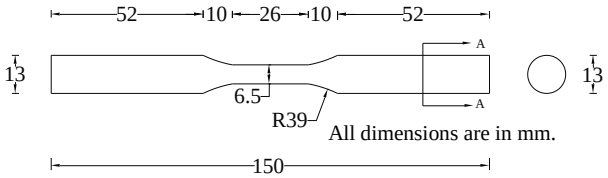

Fig. 1 Details of low cycle fatigue specimen

view of the specimen. Studies were carried out at six different strain amplitude values of ±1.10%, ±1.25%, ±1.40%, ±1.55%, ±1.70% and ±1.85%. Based on the standard practice prescribed by ASTM, the tests were carried out under constant amplitude cyclic triangular waveform loading. The test frequency was maintained in the range of 0.25 Hz to 0.50 Hz. During the tests, the applied strain, corresponding load and the number of cycles were continuously recorded using a computerised data logging system. Stress-strain hysteresis curves were obtained throughout the entire duration of the tests. The tests were continued till the specimens failed and the corresponding number of loading cycles were recorded. Fig. 4 shows the final failure of the specimen

IV. Cyclic Plastic Deformation and Stress-strain Behaviour

The stress-strain behavior obtained from a monotonic test can be quite different from that obtained under cyclic loading. This was first observed by Bauschinger. His experiments indicated the yield strength in tension or compression was reduced after applying a load of the opposite sign that caused inelastic deformation. Thus, one single reversal of inelastic strain can change the stress-strain behaviour of metals. When a material is subjected to completely reversed cyclic strain amplitudes of constant magnitude, it may exhibit (i) cyclically stable behaviour, (ii) cyclically hardening behaviour, (iii) cyclically softening behaviour and (iv) complex cyclic behaviour. If the stress magnitude required to apply the constant strain cycles remains constant, then the material is cyclically stable.

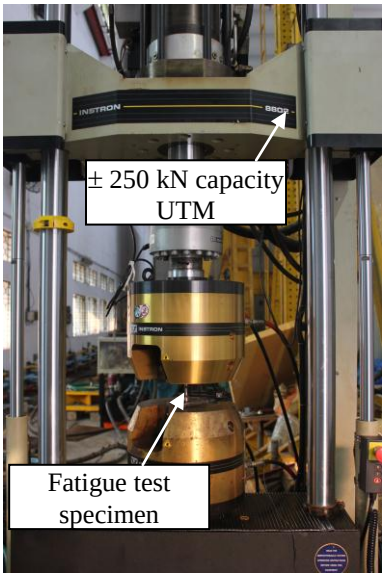

Fig. 2 Set-up for strain-controlled fatigue test

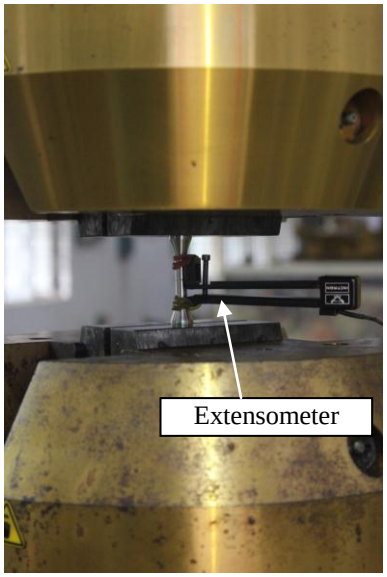

Fig. 3 Close-up view of the specimen

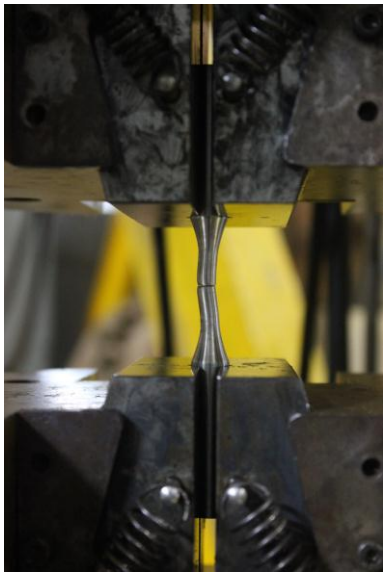

Fig.4 Close-up view of the specimen after failure

If the stress increases, the material cyclically hardens; if it decreases, the material cyclically softens. The material exhibits complex cyclic behaviour when cyclic softening, hardening, or stable behaviour occurs for different strain ranges. The material usually exhibits an initial transient behaviour, but reaches an essentially cyclically stable stress-strain behaviour that corresponds to a constant hysteresis curve. This stable behaviour is usually reached at about 50% of the fatigue life (mid-life) of the material. Fig. 5 shows a typical cyclically stable stress-strain hysteresis curve. The width of the curve at zero stress is the true plastic strain range ($\Delta\varepsilon_p$) and the height of the loop is the true stress range ($\Delta\sigma$).

The total strain amplitude ($\Delta\varepsilon/2$) for a completely reversed, strain-controlled test may be expressed as Equation (1):

$$\Delta\varepsilon/2 = \Delta\sigma/2E + \Delta\varepsilon_p/2 \quad (1)$$

where

$$\Delta\sigma/2 = K'\left(\Delta\varepsilon_p/2\right)^{n'} \quad (2)$$

The cyclic stress-strain curve may be expressed by the Constitutive Equation (3) as:

$$\Delta\varepsilon/2 = \Delta\sigma/2E + \left(\Delta\sigma/2K'\right)^{1/n'} \quad (3)$$

The true stress amplitude ($\Delta\sigma/2$) and reversals to failure ($2N_f$) are related, using the Basquin's law expressed in Equation (4) as:

$$\Delta\sigma/2 = \sigma_f'\left(2N_f\right)^b \quad (4)$$

The true plastic strain amplitude ($\Delta\varepsilon_p/2$) and the reversals to failure ($2N_f$) are related, using the Coffin-Manson's law expressed in Equation (5) as:

$$\Delta\varepsilon_p/2 = \varepsilon_f'\left(2N_f\right)^c \quad (5)$$

Using the Basquin's and Coffin-Manson's laws the total strain amplitude is expressed in Equation (6) as:

$$\Delta\varepsilon/2 = \sigma_f'/E\left(2N_f\right)^b + \varepsilon_f'\left(2N_f\right)^c \quad (6)$$

where

N_f = cycles to failure
E = Young's modulus
K' = cyclic strength coefficient
n' = cyclic strain hardening exponent
σ_f' = fatigue strength coefficient
b = fatigue strength exponent
ε_f' = fatigue ductility coefficient and
c = fatigue ductility exponent

Fig. 6 shows a typical log-log plot of strain amplitude versus reversals to failure. At a lower value of fatigue life, the plastic strain amplitude is large compared to the elastic strain amplitude; at a higher value of fatigue life, the elastic strain amplitude is large compared to the plastic strain amplitude. The fatigue life, at which the total strain amplitude consists of equal elastic and plastic strain amplitude components, is called as transition fatigue life ($2N_t$).

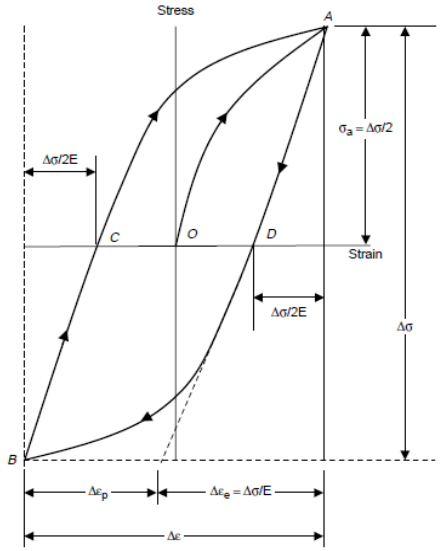

Fig. 5 Cyclically stable stress-strain hysteresis curve

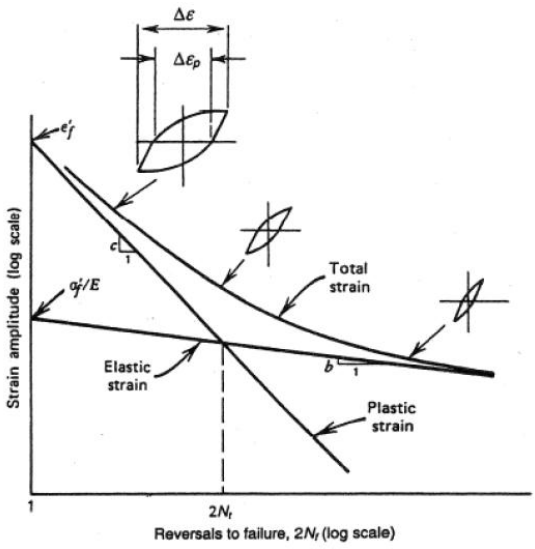

Fig. 6 Representation of fatigue life relationships

V. Results and Discussions

The number of cycles to failure for the specimens tested at strain amplitude values of ±1.10%, ±1.25%, ±1.40%, ±1.55%, ±1.70% and ±1.85% were 342, 257, 186, 148, 135 and 92 respectively. Fig. 7 shows the typical stress-strain hysteresis curves for ±1.25% strain amplitude at different cycles of loading. Fig. 8 shows the stabilized stress vs. strain hysteresis curves for six different strain amplitudes. Fig. 9 shows the loading portion of the stabilized hysteresis curves compared with the monotonic loading curve. Using cyclically stable stress-strain curves obtained at 50% of the fatigue life of the specimens, true plastic strain range and true stress range values were obtained. Table II gives the cyclic stress-strain

components. Based on the test results, empirical relationships have been obtained between the cyclic variables of stress, total strain, plastic strain and fatigue life. Based on the empirical relationships, using the values of stress-strain components and reversals to failure, fatigue parameters for the material have been evaluated.

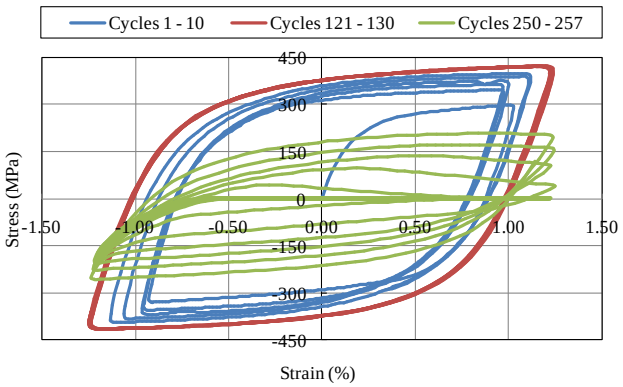

Fig. 7 Typical stress-strain hysteresis curves for ±1.25% strain amplitude

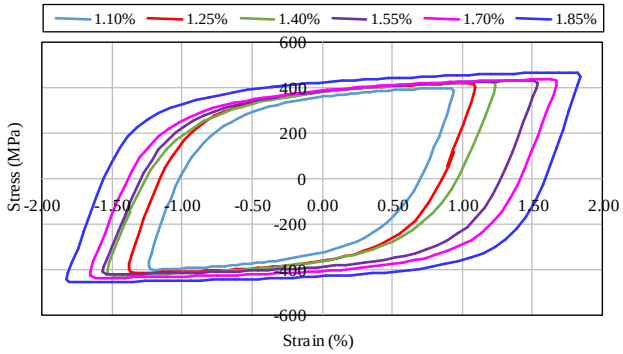

Fig. 8 Stabilized stress vs. strain hysteresis curves for six different strain amplitudes

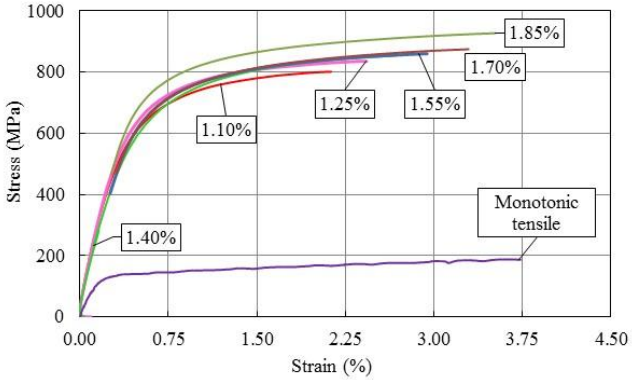

Fig. 9 Loading portion of the stabilized hysteresis curves compared with monotonic loading curve

Table III gives values of fatigue parameters for the material SA 312 Type 304LN. The table also gives values of these parameters for the material SS 304L, for the purpose of comparison, as reported by Julie Colin et al. [14]. These fatigue parameters will be useful in determining the number of cycles for fatigue-ratcheting crack initiation in components made of this material.

A. *Evaluation of* K' *and* n'

A log-log plot of true stress amplitude versus true plastic strain amplitude was obtained in order to evaluate the cyclic strength coefficient, K' and cyclic strain hardening exponent, n' as shown in Fig. 10. A power law relationship in the form of Eq (2) has been fit and the values for K' and n' were obtained as 414.66 and 0.2048 respectively.

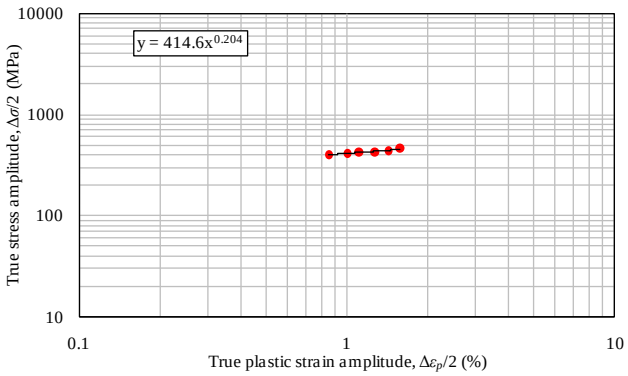

Fig. 10 True stress range versus true plastic strain range

B. *Evaluation of* σ_f' *and b*

A log-log plot of true stress amplitude versus the number of reversals to failure was obtained in order to evaluate the fatigue strength coefficient, σ_f' and fatigue strength exponent, *b* as shown in Fig. 11. A power law relationship in the form of Eq (4) has been fit and the values for σ_f' and *b* were obtained as 777.54 and -0.1010.

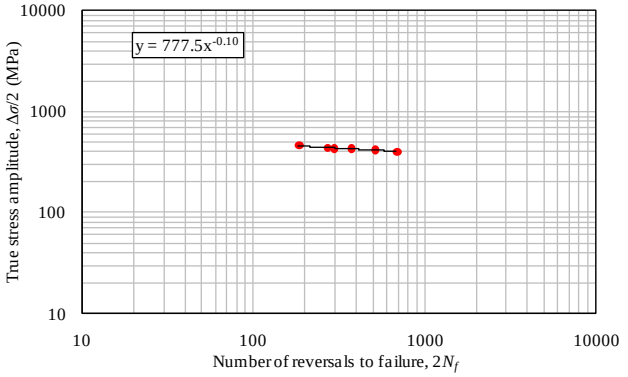

Fig. 11 True stress range versus reversals to failure

C. *Evaluation of* ε_f' *and c*

A log-log plot of true plastic strain amplitude versus the number of reversals to failure was obtained to evaluate the fatigue ductility coefficient, ε_f' and fatigue ductility exponent, *c* as shown in Fig. 12. A power law relationship in the form of Eq (5) has been fit and the values for ε_f' and *c* were obtained as 0.1955 and -0.4780 respectively.

TABLE II. CYCLIC STRESS-STRAIN COMPONENTS

Sl. No.	Specimen ID	Total strain amplitude (%)	True Plastic strain amplitude, $\Delta\varepsilon_p/2$ (%)	True stress range, $\Delta\sigma$ (MPa)	Number of reversals to failure ($2N_f$)
1	LCF 13-1	±1.10	0.856	400.687	684
2	LCF 13-2	±1.25	1.004	417.468	514
3	LCF 13-3	±1.40	1.107	427.224	372
4	LCF 13-4	±1.55	1.273	430.585	296
5	LCF 13-5	±1.70	1.429	437.379	270
6	LCF 13-6	±1.85	1.577	463.874	184

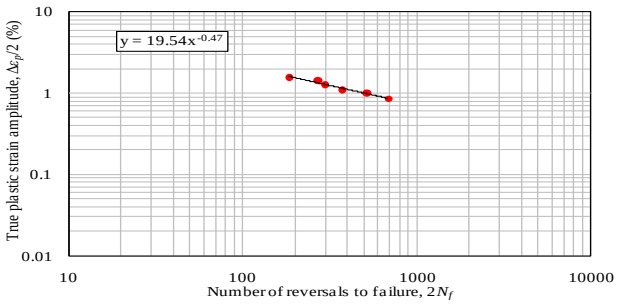

Fig. 12 True plastic strain range versus reversals to failure

TABLE III. FATIGUE PARAMETERS

Fatigue parameters	SA 312 Type 304LN	SS 304L [14]
Cyclic strength coefficient, K' (MPa)	414.66	434/4742 (bilinear fit)
Cyclic strain hardening exponent, n'	0.2048	0.1106/0.5121 (bilinear fit)
Fatigue strength coefficient, σ'_f (MPa)	777.54	330/1890 (bilinear fit)
Fatigue strength exponent, b	-0.1010	-0.0373/-0.2040 (bilinear fit)
Fatigue ductility coefficient, ε'_f	0.1955	0.1325
Fatigue ductility exponent, c	-0.4780	-0.3738

VI. SUMMARY AND CONCLUSIONS

In order to determine the fatigue parameters for SA 312 Type 304LN stainless steel, low cycle fatigue tests were carried out under strain control at different strain amplitudes of ±1.10%, ±1.25%, ±1.40%, ±1.55%, ±1.70% and ±1.85%. From the cyclically stable stress-strain curves obtained at 50% of the fatigue life of the specimens, true plastic strain range and true stress range values were obtained. Using the empirical relationships, fatigue parameters, namely cyclic strength coefficient, cyclic strain hardening exponent, fatigue strength coefficient, fatigue strength exponent, fatigue ductility coefficient and fatigue ductility exponent were evaluated; the values of the same were found to be 414.66 MPa, 0.2048, 777.54 MPa, -0.1010, 0.1955 and -0.4780 respectively. These fatigue parameters will be useful in determining the number of loading cycles for fatigue-ratcheting crack initiation in components made of this material.

ACKNOWLEDGMENT

The first author thanks the Director, CSIR-SERC, Chennai for permitting him to carry out his M.E. project work at CSIR-SERC, based on which this paper has been prepared. The authors from CSIR-SERC thank Director and Advisor (Management), CSIR-SERC for the constant support and encouragement extended to them in their R&D activities. This paper is published with the kind permission of the Director, CSIR-SERC, Chennai.

REFERENCES

[1] Lim Jae-Yong, Hong Seong-Gu, and Lee Soon-Bok, "Application of local stress-strain approaches in the prediction of fatigue crack initiation life for cyclically non-stabilized and non-Masing steel," International Journal of Fatigue, Vol. 27, 2005, pp. 1653-1660.

[2] A. Dutta, S. Dhar, and S.K. Acharyya, "Material characterization of SS 316 in low cycle fatigue loading," J. of Mat. Sci, Vol. 45, No. 7, 2010, pp. 1782-1789.

[3] J. Shit, S. Dhar, and S. Acharyya, "Modeling and finite element simulation of low cycle fatigue behaviour of 316 stainless steel," Journal of Procedia Engineering, Vol. 55, 2013, pp. 774-779.

[4] J. Rider, S.J. Harvey, and H.D. Chandler, "Fatigue ratcheting and interactions," International Journal of Fatigue, Vol. 17, No. 5, 1995, pp. 507-511.

[5] E. Weiß, B. Postberg, T. Nicak, and J. Rudolph, "Simulations of ratcheting and low cycle fatigue," International Journal of Pressure Vessels and Piping, Vol. 81, No. 3, 2004, pp. 235-242.

[6] X. Lu, "Influence of residual stress on fatigue failure of welded joints," Ph.D. Thesis, North Carolina State University, February 2003.

[7] Shaquille Bari, and Tasnim Hassan, "Anatomy of coupled constitutive models for ratcheting simulation," International Journal of Plasticity, Vol. 16, Nos. 3-4, 2000, pp. 381-409.

[8] Sumit Goyal, S.K. Gupta, S. Sivaprasad, S. Tarafder, V. Bhasin, K.K. Vaze, and A.K. Ghosh, "Low cycle fatigue and cyclic plasticity behavior of Indian PHWR/AHWR primary piping material," Journal of Procedia Engineering, Vol. 55, 2013, pp. 136-143.

[9] Bhavana Joy, S. Vishnuvardhan, G. Raghava, P. Gandhi, and M. Paul Mathews, "Low cycle fatigue characteristics of SS 304LN stainless steel," Proceedings of the 2nd International Conference on Materials. for the Future, February 23-25, 2011 (in CD).

[10] S. Vishnuvardhan, G. Raghava, and M. Saravanan, "Low cycle fatigue and ratcheting studies on SA 312 Type 304LN stainless steel," Proceedings of the 1st World Conference on Fracture and Damage Mechanics, Mahatma Gandhi University, Kottayam, Kerala, August 09-11, 2014 (in CD).

[11] ASTM A312 / A312M - 14, "Standard specification for seamless, welded and heavily cold worked austenitic stainless steel pipes," ASTM International, USA, 2014.

[12] ASTM E8 / E8M - 13a, "Standard test methods for tension testing of metallic materials," ASTM International, USA, 2013.

[13] ASTM E606 / E606M - 12, "Standard test method for strain-controlled fatigue testing," ASTM International, USA, 2012.

[14] J. Colin, A. Fatemi, and S. Taheri, "Fatigue behaviour of stainless steel 304L including strain hardening, prestraining, and mean stress effects," Journal of Engineering Materials and Technology, Vol. 132, 2010, pp. 1-13.